Macromolecules

Cite This: Macromolecules 2019, 52, 4666−4672

Article

pubs.acs.org/Macromolecules

# Electrokinetics in Viscoelastic Liquid Electrolytes above the Diffusion Limit

Alexander Warren,[†] Duhan Zhang,[‡] Snehashis Choudhury,[†] and Lynden A. Archer*[,†]

[†]School of Chemical and Biomolecular Engineering and [‡]School of Mechanical and Aerospace Engineering, Cornell University, Ithaca, New York 14853, United States

Supporting Information

**ABSTRACT:** Electrodeposition of metals at planar electrodes is known to be fundamentally unstable in liquid electrolytes driven at high ionic currents. The instability is thought to arise from unstable hydrodynamics at the electrode/electrolyte interface but may ultimately couple to underlying morphological instabilities to enhance the growth of ramified, three-dimensional structures, including dendrites. Here, we experimentally study the effect of high-molar-mass polymers on transport properties of liquid electrolytes and investigate the effect of electrolyte viscoelasticity in regulating the hydrodynamic instability known as electroconvection. Experiments performed in electrolytes bounded either by cation-selective polymer membranes or metallic electrodes make it possible to decouple hydrodynamic and morphological instabilities for the first time. Through indirect electrokinetic and direct tracer particle visualization studies, we find that high-molecular-weight polymers are effective in suppressing hydrodynamic instabilities in liquid electrolytes, particularly when the polymers are long enough to entangle. Direct visualization experiments reveal further that even at modest fields, electroconvection occurs on multiple length scales, and entangled liquid electrolytes reduce convection throughout the length scale range accessible to our experiments.

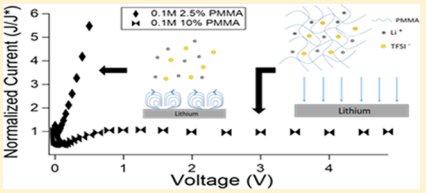


## INTRODUCTION

Electrodeposition of metals is a fundamentally unstable process at high ionic currents. Its stability has been studied for over 100 years in the context of electroplating[1] but has re-emerged in recent years as a crucial impediment to next-generation batteries that utilize high-capacity, energetic metals, such as zinc, aluminum, and lithium, as anodes. At high rates, recharge of any of these metals produces concentration polarization in liquid electrolytes, which is known to drive a hydrodynamic instability termed electroconvection. Early work has shown that the instability causes nonuniform transport of metal cations to the interface, leading to the rough electrodeposits loosely termed dendrites during battery charging.[2−4] Concentration polarization in an electrochemical cell is a consequence of the selective reduction of cations at the anode surface, which depletes cations from the electrolyte. Local charge balance requires diffusion of cations from elsewhere in the cell to compensate the depleted charge. Charging a battery at current densities that exceed the diffusion limit, therefore, produces a region near the electrode termed the extended space charge regime, in which electroneutrality cannot be maintained at all times,[4,5] and which extends much further into the electrolyte bulk than the equilibrium space charged formed at the interface between any charged substrate in an electrolyte.

A similar process has been studied at interfaces formed between cation-selective/exchange membranes that restrict the passage of anions.[6] In this latter case, the formation of the space charge is decoupled from the boundary condition at the interface, and the consequences of the space charge region on the local electric field, fluid trajectories, and ion migration profiles can be analyzed in greater detail. On the basis of theory,[7,8] numerical simulations,[9,10] and a limited set of experiments,[11,12] current thinking is that the large and nonuniform electric field required to maintain an imposed current/ion flux through the space charge region couples with the charged fluid to create a body force that drives fluid motion in the cell. This force is analogous to that which drives electro-osmotic flow in any electrolyte when an external electric field interacts with the equilibrium space charge formed at an electrified interface immersed in a liquid electrolyte, and the convective rolls it produces have been termed electro-osmotic flow of the second kind.[7,13] Because electroconvective rolls preferentially transport ions to the tips of dendrites and increase the roughness of electrodeposits,[2,8,14] they also exacerbate morphological instabilities known to produce rough dendritic electrodeposition of metals.

Polarization of the ion distribution in a liquid electrolyte produces density gradients in the electrolytes, which under the action of gravity can complicate the experimental analysis of electroconvection. The orientation of gravity relative to the electric field provides a relatively straightforward empirical constraint for limiting/increasing the influence of gravity.[15] In the gravitationally stable configuration, the imposed electric field in the cell is opposite to gravity, meaning that density gradients limit the extension of electroconvective flow patterns. The opposite is true for the gravitationally unstable

Received: March 18, 2019
Revised: May 20, 2019
Published: June 7, 2019







DOI: 10.1021/acs.macromol.9b00536
Macromolecules 2019, 52, 4666−4672

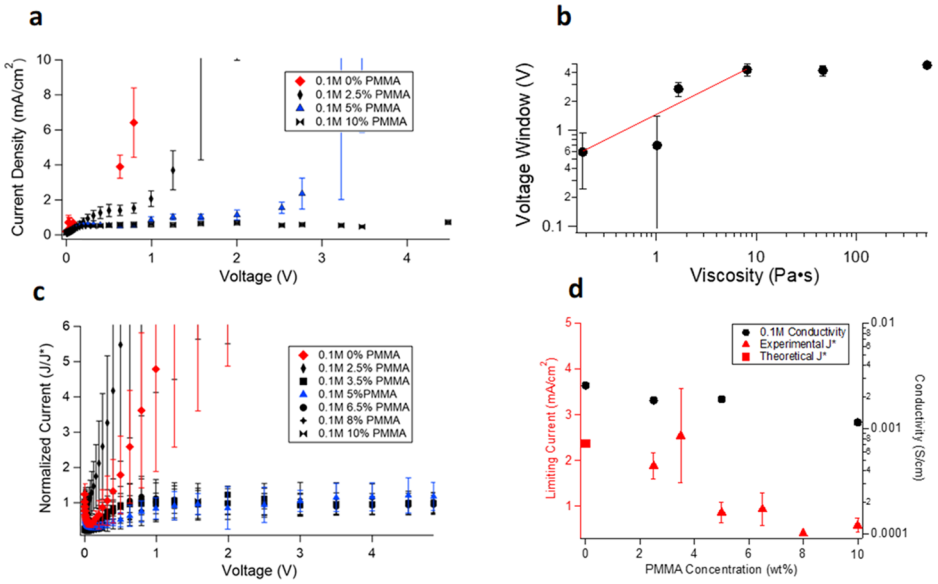


**Figure 1.** (a) Current voltage diagrams obtained using symmetric lithium Li||Li cells and aprotic liquid electrolytes with varying PMMA concentration. Even at relatively low PMMA concentrations, large enhancements of the width of the diffusion-limited ion-transport plateau are observed. (b) The voltage window or length of the plateau region from the current voltage diagram is plotted as a function of the electrolyte viscosity. The red line is a best-fit to the data and supports the relationship $\Delta V \sim \eta^{0.5}$. (c) Current voltage diagrams obtained using Li||Cu cells with an ion-selective membrane used to isolate hydrodynamic effects from morphological changes at the electrode. (d) The conductivity and limiting current measured as functions of the polymer concentration. It is evident that although the bulk conductivity of the electrolyte remains relatively constant, the limiting current is largely reduced at polymer concentrations above the entanglement threshold (~5%).

configuration, in which gravity can facilitate the destabilization of electroconvection. The importance of gravitational forces relative to the viscous forces that must be overcome to produce fluid motion as a result of ion electromigration can be quantified in terms of the nondimensional Rayleigh number, $Ra = \beta \Delta c g L^3/\nu D$. Here, $\beta$ is the solute expansion coefficient, $L$ is the gap between the electrodes of interest, $g$ is the acceleration due to gravity, $\Delta c$ is the change in the concentration, and $\nu$ and $D$ are the kinematic viscosity and diffusion coefficient, respectively. For Rayleigh numbers greater than a critical value of approximately 1000, gravitational effects cannot be ignored.

Here, we investigate the effects of high-molecular-weight polymer additives on the stability of this second kind electroosmotic flow. Our study is motivated by recent experiments by Wei et al.,[16] which show that at concentrations as low as 4% by weight, high-molecular-weight polymer additives in liquid electrolytes impart viscoelasticity to the electrolytes, which suppress hydrodynamic instability during recharge of a metal electrode in liquid electrolytes. Here, we wish to remove complications arising from changes in the boundary condition at an advancing metal electrodeposit front, to facilitate more detailed understanding of the role electrolyte viscoelasticity plays in regulating electroconvection at interfaces formed between an ion-selective membrane and liquid electrolyte. As in the study by Wei et al.,[16] we will show that at sufficiently high polymer additive molecular weights where polymer chains entangle in the solution, the polymer additive has a much larger effect on momentum transport in the electrolyte, in comparison to its impact on ion transport. The large increase in the viscosity and elasticity imparted by the polymer is further shown to extend the limiting current plateau in electrokinetics experiments and dramatically reduce the intensity of electroconvective flows. Both effects are, in turn, shown to be insensitive to electrolyte or polymer chemistry. Our results, therefore, imply that provided the selected polymer additive is electrochemically stable at the measurement conditions, any long-chain polymer with the ability to entangle at low concentrations to maintain high ionic conductivities while imparting viscoelasticity to the electrolyte should suffice.

## RESULTS AND DISCUSSION

Aprotic liquid electrolytes composed of a 1:1 volume ratio mixture of ethylene carbonate (EC) and propylene carbonate (PC) containing 0.1 and 1 M lithium bis(trifluoromethane)-sulfonimide salt were used in the majority of the studies reported in this paper. An electrochemically inert polymer poly(methyl methacrylate) (PMMA) ($M_w$ = 0.996 × $10^6$ g/mol) was dissolved in these electrolytes to create viscous liquids with polymer concentrations up to 10 percent by weight. Electrokinetics in the resultant viscoelastic liquid electrolytes was studied in two electrochemical cell geometries: (i) symmetric Li||Li cells (Figure S1a) in which PTFE (Teflon) washers with a thickness of 0.8 mm were used as spacers between the electrodes and (ii) asymmetric Li||Cu cells (Figure S2a), in which a Nafion NRE 212 cation-selective membrane (Sigma-Aldrich) was placed on the top of the copper-facing side of the PTFE washer. In either geometry, current voltage profiles were recorded from time-dependent voltage ramp measurements using a Maccor Series 4000 Battery Tester. Rheological properties of all electrolytes used in the study were investigated in a small-amplitude oscillating shear using an Anton Paar MCR Rheometer outfitted with a 50 mm-diameter cone and plate fixtures with a fixed cone angle of approximately 1°. The direct current (DC) ionic conductivity of the electrolytes was measured as a function of the polymer concentration using a Novocontrol N40 Broadband Dielectric Spectrometer at temperatures in the range 10−95 °C. Electrokinetics studies were complemented with flow visual-



DOI: 10.1021/acs.macromol.9b00536
Macromolecules 2019, 52, 4666−4672

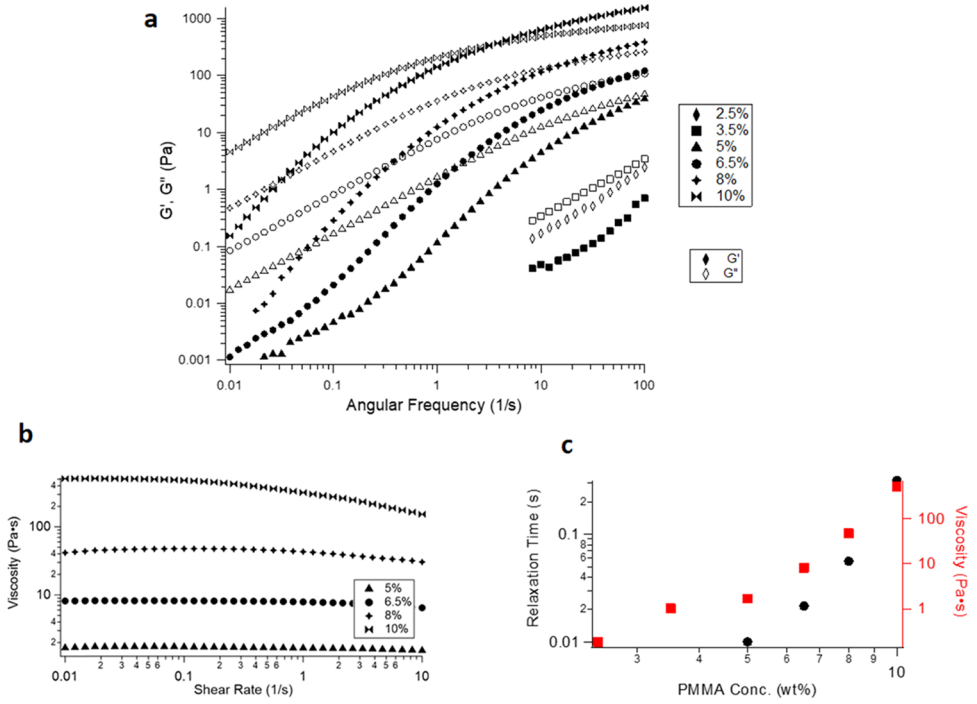


**Figure 2.** (a) Frequency-dependent storage ($G'$) and loss ($G''$) moduli deduced from small-amplitude oscillatory shear rheology measurements using 0.1 M LiTFSI in EC/PC aprotic liquid electrolyte with varying PMMA concentration. The $G'$ for the electrolyte containing 2.5% PMMA are not shown because the measured values are below the detection limit of the rheometer used in the study. (b) Shear rate sweep rheology of the same electrolytes demonstrating that as the polymer concentration increases, there is a transition from Newtonian to non-Newtonian shear-thinning rheological behavior. (c) The dependence of electrolyte relaxation time and viscosity as a function of the polymer concentration.

ization of polystyrene tracer particles (average diameter = 10 $\mu$m) dispersed in aqueous 10 mM $CuCl_2$ electrolytes containing 0, 0.5, and 1 wt % of an ultra-high-molecular-weight poly(ethylene oxide) (PEO) ($M_w$ = 8 × $10^6$ g/mol). Measurements were performed in an optical cell (Figure S4a) composed of 0.55 mm-thick copper electrodes at a fixed gap separation of 1.25 cm. Voltage control for these experiments was achieved using a Neware CT-3008 Battery Tester.

We investigated electrokinetics in the aprotic liquid electrolytes by recording the current−voltage ($i$−$V$) profiles as a function of the polymer concentration. In these tests, a longer plateau in the diffusion-limited regime signals a suppression of convection. On this basis, we show later that it is possible to extend that stable voltage window to arbitrarily high values (in many cases to values outside the electrochemical stability window of the electrolyte solvent) by simply increasing the concentration of the polymer. Our goal is to perform experiments where transport effects dominate electrochemical changes at the electrodes, which requires conditions where the diffusion boundary layer thickness spans much of the interelectrode space. To achieve such conditions, we imposed voltages in the range of 0−5 V (the upper limit for electrolyte breakdown) in a step-ramp protocol (each step lasted for 5 min, see Figure S1) and recorded the average current at the end of each step.

The cell configuration depicted in Figure S1 was used to represent a system in which morphological changes associated with metal deposition influence the boundary conditions experienced by an electrolyte in the electrokinetics studies. This couples both the hydrodynamic and morphological instabilities associated with the high current electrodeposition of metals. These experiments were complemented with others in a second cell configuration (see Figure S2), in which a lithium metal counter electrode was used as a supply of lithium ions and a Nafion membrane used as a cation-selective membrane, to achieve ion depletion without the possibility of morphological instabilities. To fully understand the extent to which a viscoelastic electrolyte can stabilize electroconvection, all cells were mounted in the gravitationally unstable configuration.

At the lower salt concentration of 0.1 M LiTFSI, the Rayleigh number is approximately unity at 10 wt % PMMA, 200 for an electrolyte with 5 wt % PMMA and 2.1 × $10^5$ for the control. The resulting $i$−$V$ curves obtained from the symmetric cell experiments are reported in Figure 1a. It is apparent that for electrolytes with polymer concentrations under 3.5 wt %, the current begins to diverge with polarization under 1 V. Furthermore, at higher polymer concentrations, the diffusion-limited plateau is seen to be extended. Figure 1b investigates the effect of electrolyte viscosity on the width $\Delta V$ of the diffusion-limited transport regime. The results show that a rough scaling relationship $\Delta V \sim \eta^{0.5}$ can be defined for the first four points, after which the voltage window is determined by the end point of the test. However, the expectation is that the effect of viscosity saturates above 5%. This two-stage relationship between $\Delta V$ and $\eta$ is also evident in the earlier study by Wei[16] but is in closer accord with expectations from our recent theoretical study of electroconvection in entangled polymers, where $\Delta V$ was shown to exhibit a progressively weaker dependence on $\eta$ (from $\Delta V \sim \eta^{0.5}$ to $V \sim \eta^0$) as the correlation length in an entangled polymer solution decreases.[17]

Figure 1c shows the results for the analogous experiment where an ion-selective membrane is employed. Here, we normalized the recorded currents by the empirical or calculated diffusion limiting current to facilitate the compar-



DOI: 10.1021/acs.macromol.9b00536
Macromolecules 2019, 52, 4666−4672

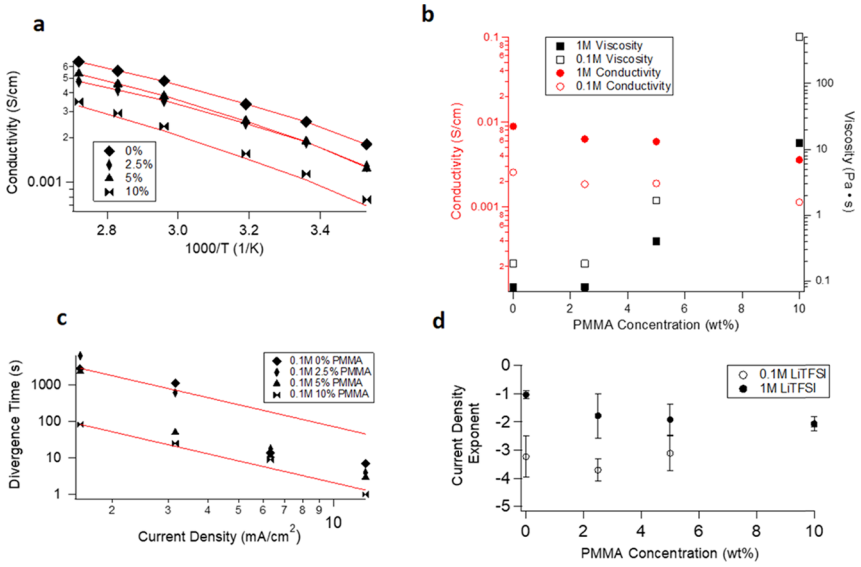


**Figure 3.** a) DC conductivity of electrolytes as a function of temperature. The red lines are VFT fits for the conductivity data. (b) Conductivity and viscosity represented as a function of the polymer concentration. It is evident that the conductivity decrease is relatively small compared with the large increase in the viscosity as the polymer concentration increases. (c) Voltage divergence time (for constant current experiments) shown as a function of current density. The red lines are guides for the theoretical relationship of $t_{div} \sim J^{-2}$. (d) Results of fitting the current density exponent for the different concentrations of polymers. Theoretically, the exponent should be −2, and this is best shown for the high polymer concentration and the 1 M concentration of salt.

isons. In this presentation, any value of the normalized current density that exceeds 1 would be defined as an overlimiting current. For polymer concentrations below 3.5 wt %, we find that overlimiting conductance proceeds essentially unchecked by electrolyte viscoelasticity; however, for PMMA concentrations of 3.5 wt % and higher, the diffusion-limited plateau is extended indefinitely (at least up to 5 V, where the electrochemical stability of the electrolyte solvent limits the experiment). Our findings imply that overlimiting conductance is essentially eliminated at an ion-selective membrane in electrolytes above the concentration, which will be shown to be near the entanglement threshold. Results reported in the Supporting Information Figure S2 show that this effect is sensitive to the electrolyte salt concentration and the PMMA concentration at which overlimiting conductance is arrested shifts to higher values at higher salt concentrations. This finding is consistent with our recent findings from direct numerical simulations of viscoelastic liquid electrolytes that the magnitude of the electroconvective slip velocity rises as the Debye screening length in the electrolyte becomes smaller.[18] We hypothesize that the polymer elasticity is effective in suppressing hydrodynamic instability, which is considered responsible for overlimiting conductance.

As the first test of this hypothesis, we compare our findings with a recent theoretical study where we employed linear stability analysis of a two-fluid polymer model to determine the effect of entangled polymers on the hydrodynamic, as well as coupled morphological and hydrodynamics, instability.[17] In qualitative agreement with the experimental observations, the theory shows that entangled polymers suppress hydrodynamic instability by selectively imposing a stronger drag on the electrolyte solvent than on ions in the solution. The support for this framework, in turn, comes from Figure 1d where we report limiting currents and conductivities for the range of polymer concentrations studied. For the control and weakly entangled electrolytes, where overlimiting conductance is strong and a clear diffusion-limited current plateau is not observed, the limiting current values correspond to the theoretical limiting current deduced from the measured electrolyte conductivity, which are generally higher than the measured values in simple Newtonian liquid electrolytes.[19,20] The results show that both the limiting current and conductivity are weaker functions of the polymer concentration than the electrolyte viscosity, consistent with the two-fluid framework upon which the linear stability analysis builds.

The physical properties of the designed electrolytes were evaluated using a suite of analytical methods. Figure 2a reports the dynamic storage ($G'$) and loss ($G''$) moduli of the electrolytes at 25 °C as a function of the polymer concentration. The analysis of the results for the 0.1 M LiTFSI electrolytes reveals that above a concentration of approximately 5 wt % of the PMMA, the loss modulus surpasses the storage modulus at a high frequency. This implies that our electrolytes transition from nominally viscous liquids ($G'' > G'$ over the full frequency range explored) to viscoelastic fluids, wherein $G' > G''$ only at higher $\omega$. The transition from liquid to viscoelastic fluid behavior can be used to infer microscopic information about the configuration of the polymer chains in the solution; it may be used, for example, to deduce that above a polymer concentration of 5 wt %, the PMMA chains form physical entanglements in the electrolyte solution.[21]

The apparent viscosity of the electrolytes was determined using a shear rate sweep rheological method in which electrolyte solutions are subjected to a constant shear rate at 25 °C, and the long-time/steady-state viscosity at each rate is measured. Results from these experiments are reported in Figure 2b and show that for polymer concentrations above 5 wt %, the electrolytes transition from a Newtonian fluid state (wherein the viscosity is independent of the shear rate) to a non-Newtonian, shear-thinning state, in which the viscosity decreases with increasing rate.



DOI: 10.1021/acs.macromol.9b00536
Macromolecules 2019, 52, 4666−4672

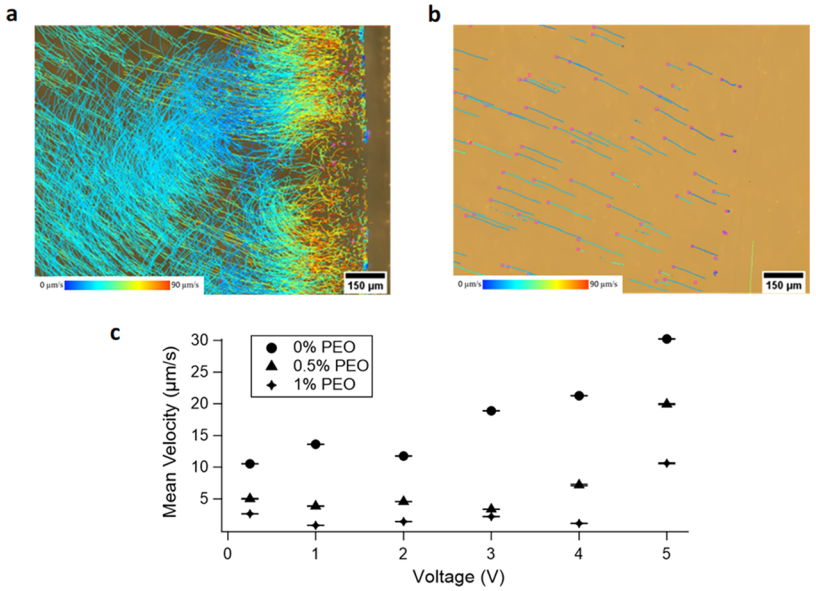


**Figure 4.** (a, b) Example velocity maps for control and 1 wt % PEO under 4 V polarization. Both maps encompass 3 min of particle tracking, which exhibits the significantly higher motion and turbulence in the control relative to the 1 wt % polymer. (c) The average particle velocity as a function of voltage for 0, 0.5, and 1 wt % PEO in the system. For each voltage, the control case has higher velocities and it is even more evident when turbulent convection sets in at 3 V.

The time scale for the polymer relaxation can be extracted from the inverse of the frequency at which the loss and storage moduli crossover in the previous oscillatory shear measurements.[22,23] Figure 2c plots this time scale and the Newtonian viscosity of the electrolytes as a function of the polymer concentration. Above the critical concentration of 5 wt %, the characteristic polymer relaxation time and viscosity follow the relationships, $\lambda \sim c^{4.91}$ and $\eta \sim c^{8.22}$, respectively. These power-law scalings are slightly higher than those reported previously[24,25] but are consistent with our microscopic picture that above a concentration of approximately 5 wt %, the PMMA chains in the electrolyte form an entanglement network that produces the large enhancements in the fluid viscosity.

The conductivities of the electrolytes are reported in Figure 3a. The solid lines through the data are best-fit curves obtained using the VFT equation;[26] the apparent activation energies extracted from the fits are reported in Figure S3 in the Supporting Information section. Comparing the effects of the polymer concentration on conductivity and viscosity (Figure 3b), it is clear that the conductivity remains relatively constant, whereas the viscosity increases significantly at high polymer concentrations. It is also significant that the activation energies deduced from the VFT fits of the temperature-dependent conductivity also remain relatively independent of the polymer concentration. We interpret these observations to mean that the polymer additives have little impact on ion motion in the system.

The most straightforward approach for characterizing ion polarization at an interface is to measure the voltage required to maintain a specified (controlled) current density as a function of time. For current densities above the diffusion limit, ion polarization causes the voltage to diverge on a certain current-density-dependent time scale termed the Sand's time[27,28]

$$t_{\text{sand}} = \pi D \frac{(z_c c_0 F)^2}{4(J t_a)^2}$$

here, $D$ is the diffusion coefficient, $z_c$ is the cation charge number, $c_0$ is the bulk concentration, $F$ is faraday's constant, $J$ is the current density, and $t_a$ is the anion transference number. The coin cell configuration depicted in the Supporting Information Figure S1a was used to characterize voltage versus time profiles. After a certain period of time, the voltage begins to diverge, an example plot is shown in the Supporting Information Figure S3. By performing these chronoamperometric measurements for electrolytes over a range of polymer concentrations and current densities, the voltage divergence time $t_{\text{div}}$ was determined for a range of electrolyte compositions and at various current densities (Figure 3c). The lines through the figure are provided as guides to the eye to aid visual comparison of the measured $t_{\text{div}}$ versus current density, with the theoretical scaling, $t_{\text{div}} \approx t_{\text{sand}} \sim J^{-2}$, expected from the definition of Sand's time at which polarization of the electrolyte leads to a deficit of ions at the electrode surface. For both salt concentrations studied, the measured $t_{\text{div}}$ is observed to decrease in proportion to the electrolyte viscosity but decreases much faster than expected from the electrolyte conductivity, implying that the Nernst−Einstein relationship breaks down in these electrolytes. More quantitative comparisons of the scaling exponents are provided in Figure 3d where it is observed that agreement between the measured and predicted exponents is the best in electrolytes with 1 M salt concentration and at higher polymer concentrations. This implies that even with the addition of polymers, at current densities above the diffusion limits, ions are depleted at the surface in an analogous manner as for the Newtonian liquid electrolyte.

As a more concrete assessment of our hypothesis that polymer elasticity suppresses hydrodynamic instability of liquid electrolytes at ion-selective interfaces, we turn to direct visualization studies of the electrolyte dynamics. For this



DOI: 10.1021/acs.macromol.9b00536
Macromolecules 2019, 52, 4666−4672

purpose, we constructed an optical cell (see Supporting Information Figure S4) and employed tracer particle velocimetry to directly analyze fluid motions near ion-selective interfaces. Because these experiments require long data collection times and large throughput of metal, they cannot be performed safely using Li electrodes. Here, we instead utilize copper as the working electrode and an aqueous copper electrolyte. The rheological properties of these electrolytes are similar to the lithium electrolytes studied (Supporting Information Figure S4) with an entanglement transition between 0.5 and 1 wt %. Experiments were performed at voltages varying from 0.25 to 5 V between copper electrodes with Nafion employed as an ion-selective, separating membrane. By visualizing particle trajectories at the electrolyte/Nafion interface over a range of voltages, it was possible to characterize how the hydrodynamic instability develops and what role electrolyte viscoelasticity plays in that development.

Example videos from 0 to 1 wt % polymer are provided in the Supporting Information section, which clearly show that strong convective motions emerge in the quiescent liquid electrolyte. The main features of this motion are illustrated in Figure 4a using maps of the particle velocity profiles for the control electrolyte at 5 V. The results clearly show that strong convective rolls develop quickly at the interfaces and that there are two distinct length scales in which the convection manifests. Large macroscopic rolls, comparable in size to the interelectrode spacing, co-exist with smaller, turbulent flow structures localized near the interface and in which the fluid velocity is higher, fluid trajectories more variable in space and time, and fluid flow lines exhibit higher curvatures. The larger roles are consistent with observations from previous direct numerical simulations by Mani's group.[9,10] These effects can be compared to those seen in Figure 4b for the same polarization but with the addition of 1 wt % PEO. For the same elapsed time (3 min), there is significantly more motion and turbulence for the control case. Visual inspection of the videos clearly shows that the electrolyte viscoelasticity has a more obvious effect on the large rolls than on the smaller, more turbulent features. To quantify this effect, we report in Figure 4c the average velocity deduced from the videos using the Trackmate software[29] at various potentials and polymer concentrations. The results demonstrate that as polymer concentration increases, the velocity of the resulting convective rolls decreases by more than 1 order of magnitude. The results show further that as the polymer concentration increases, a higher voltage is required to initiate electroconvection, which explains the extension of the diffusion-limited ion-transport regime observed in the previously shown $i-V$ curve.

## CONCLUSIONS

Next-generation batteries that contain metal anodes require electrolytes that have high conductivities are chemically and thermally stable at high voltages and which provide fundamental mechanisms for stabilizing intrinsically unstable electrodeposition at high current densities. We report that the addition of high-molecular-weight polymers to either aprotic liquid or aqueous electrolytes provides a facile method for imparting viscoelasticity to these electrolytes while minimally impacting conductivity. At moderate polymer concentrations, analysis of the $i-V$ curve for viscoelastic electrolytes bounded either by metal or ion-selective polymer interfaces shows that the diffusion-limited transport regime can be extended indefinitely, and that overlimiting conductance can be completely suppressed in electrochemical systems where coupling between morphological and hydrodynamic instability is eliminated. Finally, by directly visualizing the motions of micron-size, neutral tracer particles in the electrolyte bulk and near ion-selective interfaces, we report that hydrodynamic instability leads to qualitatively different electroconvective flows on small and large length scales. We also find that the average fluid velocity in an entangled polymer electrolyte is lowered by more than 1 order of magnitude, with the largest suppression occurring at the highest cell voltages where hydrodynamic instability is the strongest.

## ASSOCIATED CONTENT

### Supporting Information

The Supporting Information is available free of charge on the ACS Publications website at DOI: 10.1021/acs.macromol.9b00536.

Electrochemical cell design to allow for free convection in the electrolyte; new cell design that was used to test current voltage curves for an ion selective membrane; resulting activation energies from fitting conductivity data with a VFT relationship (PDF)

0, 0.5, 1 wt % PEO additives all under 5 V polarization (AVI) (AVI) (AVI)

## AUTHOR INFORMATION


### Corresponding Author

*E-mail: laa25@cornell.edu.

### ORCID

Duhan Zhang: 0000-0001-9428-956X

Lynden A. Archer: 0000-0001-9032-2772


### Author Contributions

A.W., S.C., and L.A.A. designed research; A.W. and D.Z. performed research; A.W. and L.A.A. analyzed data and wrote the paper.

### Notes

The authors declare no competing financial interest.

## ACKNOWLEDGMENTS

This work was supported by the Department of Energy Basic Energy Sciences Program through award #: DE-SC0016082.

## REFERENCES


(1) Bancroft, W. D. The Chemistry of Electroplating. *J. Phys. Chem.* **1905**, *9*, 277−296.

(2) Barkey, D. P.; et al. The role of induced convection in branched electrodeposit morphology selection. *J. Electrochem. Soc.* **1994**, *141*, 1206−1212.

(3) Rosso, M.; et al. Experimental evidence for gravity induced motion in the vicinity of ramified electrodeposits. *Electrochim. Acta* **1994**, *39*, 507−515.

(4) Huth, J. M.; et al. Role of convection in thin-layer electrodeposition. *Phys. Rev. E* **1995**, *51*, 3444−3458.

(5) Block, M.; Kitchener, J. A. Polarization phenomena in commercial ion-exchange membranes. *J. Electrochem. Soc.* **1966**, *113*, 947−953.

(6) Chazalviel, J. N. Electrochemical aspects of the generation of ramified metallic electrodeposits. *Phys. Rev. A* **1990**, *42*, 7355−7367.

(7) Zaltzman, B.; Rubinstein, I. Electro-osmotic slip and electroconvective instability. *J. Fluid Mech.* **2007**, *579*, 173−226.

(8) Fleury, V.; Kaufman, J.; Hibbert, B. Evolution of the space-charge layer during electrochemical deposition with convection. *Phys. Rev. E* **1993**, *48*, 3831−3840.




DOI: 10.1021/acs.macromol.9b00536
*Macromolecules* 2019, 52, 4666−4672

(9) Davidson, S. M.; Wessling, M.; Mani, A. On the Dynamical Regimes of Pattern-Accelerated Electroconvection. *Sci. Rep.* **2016**, *6*, No. 22505.
(10) Demekhin, E. A.; Nikitin, N. V.; Shelistov, V. S. Direct numerical simulation of electrokinetic instability and transition to chaotic motion. *Phys. Fluids* **2013**, *25*, No. 122001.
(11) de Valença, J. C.; Wagterveld, R. M.; Lammertink, R. G. H.; Tsai, P. A. Dynamics of microvortices induced by ion concentration polarization. *Phys. Rev. E* **2015**, *92*, No. 031003.
(12) Nam, S.; et al. Experimental verification of overlimiting current by surface conduction and electro-osmotic flow in microchannels. *Phys. Rev. Lett.* **2015**, *114*, No. 114501.
(13) Rubinstein, I.; Zaltzman, B. Electro-osmotically induced convection at a permselective membrane. *Phys. Rev. E* **2000**, *62*, 2238−2251.
(14) Nishida, T.; Nishikawa, K.; Rosso, M.; Fukunaka, Y. Optical observation of Li dendrite growth in ionic liquid. *Electrochim. Acta* **2013**, *100*, 333−341.
(15) Karatay, E.; et al. Coupling between buoyancy forces and electroconvective instability near ion-selective surfaces. *Phys. Rev. Lett.* **2016**, *116*, No. 194501.
(16) Wei, S.; et al. Stabilizing electrochemical interfaces in viscoelastic liquid electrolytes. *Sci. Adv.* **2018**, *4*, No. eaao6243.
(17) Tikekar, M. D.; et al. Electroconvection and Morphological Instabilities in Potentiostatic Electrodeposition across Liquid Electrolytes with Polymer Additives. *J. Electrochem. Soc.* **2018**, *165*, A3697−A3713.
(18) Li, G.; et al. Electroconvection in a viscoelastic electrolyte. *Phys. Rev. Lett.* **2019**, *122*, No. 124501.
(19) Maletzki, F.; Rösler, H.-W.; E. Staude, E. Ion transfer across electrodialysis membranes in the overlimiting current range: Stationary voltage current characteristics and current noise power spectra under different conditions of free convection. *J. Membr. Sci.* **1992**, *71*, 105−116.
(20) Rubinshtein, I.; Zaltzman, B.; Pretz, J.; Linder, C. Experimental verification of the electroosmotic mechanism of overlimiting conductance through a cation exchange electrodialysis membrane. *Russ. J. Electrochem.* **2002**, *38*, 853−863.
(21) Tung, C.-Y.; Dynes, P. J. Relationship between viscoelastic properties and gelation in thermosetting systems. *J. Appl. Polym. Sci.* **1982**, *27*, 569−574.
(22) Volpert, E.; Selb, J.; Candau, F. Associating behaviour of polyacrylamides hydrophobically modified with dihexylacrylamide. *Polymer* **1998**, *39*, 1025−1033.
(23) Castelletto, V.; et al. Rheological and structural characterization of hydrophobically modified polyacrylamide solutions in the semi-dilute regime. *Macromolecules* **2004**, *37*, 1492−1501.
(24) Berry, G. C.; Fox, T. G. The viscosity of polymers and their concentrated solutions. *Adv. Polym. Sci.* **1968**, *5*, 261−357.
(25) Cho, J.; et al. Viscoelastic properties of chitosan solutions: Effect of concentration and ionic strength. *J. Food Eng.* **2006**, *74*, 500−515.
(26) Souquet, J.-L.; Duclot, M.; Levy, M. Salt-polymer complexes: strong or weak electrolytes? *Solid State Ionics* **1996**, *85*, 149−157.
(27) Bai, P.; Li, J.; Brushett, F. R.; Bazant, M. Z. Transition of lithium growth mechanisms in liquid electrolytes. *Energy Environ. Sci.* **2016**, *9*, 3221−3229.
(28) Sand, H. J. S. On the concentration at the electrodes in a solution, with special reference to the liberation of hydrogen by electrolysis of a mixture of copper sulphate and sulphuric acid. *Philos. Mag.* **1901**, *1*, 45−79.
(29) Tinevez, J.-Y.; et al. TrackMate: An open and extensible platform for single-particle tracking. *Methods* **2017**, *115*, 80−90.



DOI: 10.1021/acs.macromol.9b00536
*Macromolecules* 2019, 52, 4666−4672